




iSIM: instant similarity†

Cite this: *Digital Discovery*, 2024, 3, 1160Kenneth López-Pérez, Taewon D. Kim and Ramón Alain Miranda-Quintana *Received 6th February 2024
Accepted 6th May 2024

DOI: 10.1039/d4dd00041b

rsc.li/digitaldiscovery

The quantification of molecular similarity has been present since the beginning of cheminformatics. Although several similarity indices and molecular representations have been reported, all of them ultimately reduce to the calculation of molecular similarities of only two objects at a time. Hence, to obtain the average similarity of a set of molecules, all the pairwise comparisons need to be computed, which demands a quadratic scaling in the number of computational resources. Here we propose an exact alternative to this problem: iSIM (instant similarity). iSIM performs comparisons of multiple molecules at the same time and yields the same value as the average pairwise comparisons of molecules represented by binary fingerprints and real-value descriptors. In this work, we introduce the mathematical framework and several applications of iSIM in chemical sampling, visualization, diversity selection, and clustering.

Introduction

Molecular fingerprints are one of the most common representations of compounds in cheminformatics. The simplest version of fingerprints is binary vectors, where the presence of a structural feature is represented by a 1 and its absence by a 0.¹ Another popular representation is molecular descriptors, which correspond to useful numbers that encode information about a molecule; commonly they can be calculated from graph theory, quantum chemistry, and topological or experimental methods, to mention some sources.² Despite their apparent differences, both descriptors and fingerprints can be used to calculate the similarity between two molecules. From a mathematical point of view, a similarity index is a metric that measures how “related” two points are in chemical space.³ Multiple similarity measurements have been reviewed and analysed, with the well-known Tanimoto coefficient (T)^{4,5} being the usual go-to in the cheminformatics community.⁶ The main point of calculating similarity measurements lies in the “molecular similarity principle”: similar molecules have similar properties/activities.⁷ This powerful idea is at the core of virtual screening,^{8–11} hit selection,¹² QSAR/QSPR modeling,^{13,14} many chemical space exploration methods,^{15,16} activity landscape description,^{17,18} diversity selection,¹⁹ clustering,^{20,21} and many more applications.

Given the fundamental role that molecular similarity plays in drug design,²² activity studies^{23,24} and, more recently, in ML and AI pipelines,^{25–27} it is not surprising that a lot of effort has been devoted to increase the efficiency of these calculations. For instance, KD-trees^{28,29} and Ball-trees³⁰ can be used to speed up

similarity searches, while packages like FPSim2 (ref. 31) and chemfp³² are superbly optimized. In most cases, the common way of quantifying similarity is by comparing two molecules. The typical way of calculating a library's similarity/diversity is calculating the average similarity of all the possible comparisons in the library, which is a computationally costly $O(N^2)$ step. At best, KD-trees can be used to estimate library diversity in an algorithm with $N \log N$ complexity.³³ This problem has received attention from the cheminformatics community, perhaps more notably in the work of Willet *et al.*^{34,35} For example, these authors proposed an $O(N)$ approximation to the cosine similarity, but despite its appeal, it was not possible to generalize it to other similarity indices.

Motivated by this problem, our group recently developed the concept of extended similarity.^{36,37} Extended similarity performs the comparison of all the molecules in a set at the same time and yields a similarity metric for the whole set. Briefly, for a matrix of size $N \times M$, where M is the size of the fingerprint or number of molecular descriptors and N the number of molecules in a set, the first step is to sum the elements column-wise, resulting in a vector, $K = [k_1, k_2, \dots, k_M]$. Each column sum, k_q , can be used to classify the column when it is compared to a threshold in the following way: (i) if $2k_q - N > \gamma$ it will be a 1-similarity column, (ii) if $N - 2k_q > \gamma$ it will be a 0-similarity column, (iii) otherwise it will count as dissimilarity. Then, using $\Delta_{k_q} = |2k_q - N|$ as an independent variable a weighting function should be used to consider partial similarity and dissimilarity, and the function should be positive and increasing. Now the variables of any similarity metric can be transformed using the sum of the weighted or non-weighted counters. The major advantage of extended similarity is that it calculates a similarity metric for the whole set much more efficiently than by using the traditional pairwise comparisons, with this calculation now scaling as $O(N)$.^{36,37}

Department of Chemistry and Quantum Theory Project, University of Florida, Gainesville, Florida 32611, USA. E-mail: quintana@chem.ufl.edu

† Electronic supplementary information (ESI) available. See DOI: <https://doi.org/10.1039/d4dd00041b>



The notion of calculating average similarity values over a set of molecules has proven to be particularly powerful over several cheminformatics tasks. For example, extended similarity has been applied to several problems like diversity selection,^{37,38} molecular dynamics simulations,^{39,40} library diversity studies,^{41–43} activity cliffs,⁴⁴ descriptor selection for the QSAR/QSPR model,⁴⁵ fingerprint evaluations,⁴⁶ and chemical space visualization.⁴⁷ However, despite these advantages, there are some drawbacks like the need for a coincidence threshold analysis to determine the best similarity/dissimilarity separation and a different numeric value than the pairwise comparisons. These limitations inspired this work where we show the mathematical framework, analysis, and cheminformatics applications of iSIM, an “instantaneous” similarity measurement for binary fingerprints and molecular descriptors that yields virtually the same value as the average pairwise similarity comparisons in a linear scaling with the number of observations.

Theory

Binary representations

Comparisons of molecular fingerprints are based on three key indicators: the number of times there is a coincidence of two “on” bits between the fingerprints (denoted by a), the number of times there is a coincidence of two “off” bits between the fingerprints (denoted by d), and the mismatches between the fingerprints, when one bit is “on” and the other is “off” (denoted by $b + c$). With these ingredients one can propose a plethora of similarity indices, which could be interpreted as such as long as they are monotonically increasing functions of a and d , and monotonically decreasing functions of $b + c$. Here, we will be concerned mainly with the Russel–Rao (RR),⁴⁸ Tanimoto (T),^{4,5} and Sokal–Michener (SM)⁴⁹ indices:

$$\text{RR} = \frac{a}{a + d + b + c} \quad (1)$$

$$\text{T} = \frac{a}{a + b + c} \quad (2)$$

$$\text{SM} = \frac{a + d}{a + d + b + c} \quad (3)$$

(Notice that, trivially, $\text{RR} \leq \text{T} \leq \text{SM}$.)

The very definition of, say, a seems to imply that when we have N molecules, we need to consider the $\binom{N}{2} = \frac{N(N-1)}{2}$ distinct pairs to check the coincidence or not of on bits. However, it is possible to access the same information in far fewer operations. The first step is to arrange all the fingerprints in a matrix, with each fingerprint corresponding to a row. Then, we just need to find the sum of each column, which generates the same vector described before. However, the key insight now is to note that the k 's are all that we need to calculate the number of times we will have coincidence or not of any type of bit. For instance, there will be $\binom{k_q}{2}$ instances in which two on

bits will coincide in column q . Likewise, there will be $\binom{N-k_q}{2}$ coincidences of off bits. Finally, the number of mismatches is $k_q(N-k_q)$. It is natural then to make the following identification (with the sums running over all bit positions):

$$a \rightarrow \sum_{q=1}^M \frac{k_q(k_q-1)}{2} \quad (4)$$

$$d \rightarrow \sum_{q=1}^M \frac{(N-k_q)(N-k_q-1)}{2} \quad (5)$$

$$b + c \rightarrow \sum_{q=1}^M k_q(N-k_q) \quad (6)$$

With this, we have everything in place to define the instantaneous similarity (iSIM) versions of the previously discussed indices, *iRR*, *iT*, and *iSM*, as:

$$\begin{aligned} i\text{RR} &= \frac{\sum_{q=1}^M \frac{k_q(k_q-1)}{2}}{\sum_{q=1}^M \left\{ \frac{k_q(k_q-1)}{2} + \frac{(N-k_q)(N-k_q-1)}{2} + k_q(N-k_q) \right\}} \\ &= \frac{\sum_{q=1}^M k_q(k_q-1)}{MN(N-1)} \end{aligned} \quad (7)$$

$$iT = \frac{\sum_{q=1}^M \frac{k_q(k_q-1)}{2}}{\sum_{q=1}^M \left\{ \frac{k_q(k_q-1)}{2} + k_q(N-k_q) \right\}} \quad (8)$$

$$\begin{aligned} i\text{SM} &= \frac{\sum_{q=1}^M \left\{ \frac{k_q(k_q-1)}{2} + \frac{(N-k_q)(N-k_q-1)}{2} \right\}}{\sum_{q=1}^M \left\{ \frac{k_q(k_q-1)}{2} + \frac{(N-k_q)(N-k_q-1)}{2} + k_q(N-k_q) \right\}} \\ &= \frac{\sum_{q=1}^M \{k_q(k_q-1) + (N-k_q)(N-k_q-1)\}}{MN(N-1)} \end{aligned} \quad (9)$$

The case of *iRR* and *iSM* is special, because $a + b + c + d = M$, the denominators in eqn (1) and (3), are always constant, equal to the number of bits in the fingerprints (a fact that we explicitly use in the 2nd, simpler, form of the *iRR* and *iSM* indices shown above). Then, we can interpret eqn (7) and (9) as effectively combining the RR and SM similarities over independent bit positions. Given the constant-denominator characteristic, it is then easy to see that the iSIM version of these indices will provide the exact average of all the pairwise RR and SM values over the given set, but at only $O(N)$ cost. *iT*, on the other hand, will not in general give exactly the same value as the average of the pairwise



Tanimoto calculations. Once again, the key is that the T denominator is not the same for arbitrary pairs of fingerprints. In this case, we can interpret iT as an $O(N)$ median approximation^{50,51} to the $O(N^2)$ average. Despite this simplification, as shown below, iT still provides superb estimates for the pairwise average over a varied set of conditions.

Real-value representations

The previous results are promising, so it is certainly desirable to extend them to more general types of molecular representations. Here, we show how this can be done for vectors of real (in principle, continuous) values. The key insight is to use inner products between the molecular “vectors” instead of the more limited a , d , and $b + c$ indicators used in the binary case. To do this we will focus on the case where the i th molecule, $X^{(i)}$, is represented by a vector of descriptors $|X^{(i)}\rangle = [x_1^{(i)}, x_2^{(i)}, \dots, x_M^{(i)}]$. Without losing any generality, these vectors are considered to be normalized: $\forall i, q: 0 \leq x_q^{(i)} \leq 1$. The main motivation behind the focus on normalized descriptors is that we can then easily define the “flipped” representation of a molecule, $|\tilde{X}^{(i)}\rangle$, as the real-value equivalent of flipping the bits of a binary representation, that is: $|\tilde{X}^{(i)}\rangle = [1 - x_1^{(i)}, 1 - x_2^{(i)}, \dots, 1 - x_M^{(i)}]$. In terms of inner products, the previously analyzed indices can be written as:

$$RR = \frac{\langle X^{(i)} | X^{(j)} \rangle}{M} \quad (10)$$

$$T = \frac{\langle X^{(i)} | X^{(j)} \rangle}{\langle X^{(i)} | X^{(i)} \rangle + \langle X^{(j)} | X^{(j)} \rangle - \langle X^{(i)} | X^{(j)} \rangle} \quad (11)$$

$$SM = \frac{\langle X^{(i)} | X^{(j)} \rangle + \langle \tilde{X}^{(i)} | \tilde{X}^{(j)} \rangle}{M} \quad (12)$$

Notice that, for simplicity, we have directly used the fact that the denominators of the RR and SM indices are constant and equal to the total length of the molecular vectors, M .

Once again, the way of writing eqn (10)–(12) seems to suggest that calculating the average of all the RR, T, or SM comparisons demands $O(N^2)$. However, we can actually calculate the sum of all the involved inner products in $O(N)$ (albeit with a larger overhead compared to the binary case).

First, for the inner products between the molecular representations, we have:

$$\langle X^{(i)} | X^{(j)} \rangle = \sum_{q=1}^M x_q^{(i)} x_q^{(j)} \quad (13)$$

Then, for the relevant inner products appearing in eqn (10)–(12):

$$\begin{aligned} \sum_{i < j} \langle X^{(i)} | X^{(j)} \rangle &= \sum_{i < j} \sum_{q=1}^M x_q^{(i)} x_q^{(j)} \\ &= \frac{1}{2} \sum_{q=1}^M \left\{ \left(\sum_i x_q^{(i)} \right)^2 - \sum_i (x_q^{(i)})^2 \right\} \end{aligned} \quad (14)$$

$$\begin{aligned} \sum_{i < j} \langle \tilde{X}^{(i)} | \tilde{X}^{(j)} \rangle &= \sum_{i < j} \sum_{q=1}^M [1 - x_q^{(i)}][1 - x_q^{(j)}] \\ &= \frac{1}{2} \sum_{q=1}^M \left\{ \left(\sum_i [1 - x_q^{(i)}] \right)^2 - \sum_i [1 - x_q^{(i)}]^2 \right\} \end{aligned} \quad (15)$$

From these expressions, it is clear that we can follow a similar route to the one taken for the binary input. First, we need to arrange all the molecular vectors in a matrix X . Then, we need to generate some related matrices: (a) the “flipped” matrix $\tilde{X} = 1 - X$, (b) the Hadamard (element-wise) squares of these matrices, X^2 and \tilde{X}^2 . That is, if the element in row i and column q in X is given by $x_q^{(i)}$, then the corresponding elements of matrices \tilde{X} , X^2 , and \tilde{X}^2 will be $1 - x_q^{(i)}$, $(x_q^{(i)})^2$, and $[1 - x_q^{(i)}]^2$, respectively. It is important to remark that since we are only taking element-wise products, generating these auxiliary matrices will only demand $O(N)$ operations. Then, the sum of the columns of matrices X and \tilde{X} gives vectors with components $\sum_i x_q^{(i)}$ and $\sum_i (1 - x_q^{(i)})$, respectively. On the other hand, the sum of the columns for the Hadamard squares gives the factors $\sum_i (x_q^{(i)})^2$ and $\sum_i (1 - x_q^{(i)})^2$. These are all the ingredients necessary to calculate the real-value iSIM similarity indices:

$$iRR = \frac{\sum_{q=1}^M \left\{ \left(\sum_i x_q^{(i)} \right)^2 - \sum_i (x_q^{(i)})^2 \right\}}{MN(N-1)} \quad (16)$$

$$iT = \frac{\frac{1}{2} \sum_{q=1}^M \left\{ \left(\sum_i x_q^{(i)} \right)^2 - \sum_i (x_q^{(i)})^2 \right\}}{(N-1) \sum_{q=1}^M \sum_i (x_q^{(i)})^2 - \frac{1}{2} \sum_{q=1}^M \left\{ \left(\sum_i x_q^{(i)} \right)^2 - \sum_i (x_q^{(i)})^2 \right\}} \quad (17)$$

$$iSM = \frac{\sum_{q=1}^M \left\{ \left(\sum_i x_q^{(i)} \right)^2 - \sum_i (x_q^{(i)})^2 \right\} + \sum_{q=1}^M \left\{ \left(\sum_i [1 - x_q^{(i)}] \right)^2 - \sum_i [1 - x_q^{(i)}]^2 \right\}}{MN(N-1)} \quad (18)$$

Once again, iRR and iSM provide the same exact results as the average of all the pairwise comparisons, due to the convenient constant denominators. For iT , this is just a median-like approximation but, as will be illustrated below with different numerical tests, eqn (17) provides an excellent approximation to the $O(N^2)$ result.

Datasets

10 000 random datasets were generated, with the number of fingerprints ranging from 100 to 1000 and the size of the



fingerprints ranging from 166 to 2048. For the binary case, to ensure that the datasets covered the complete range of the similarity index domains, each dataset was randomly biased to have different proportions of ones and zeros. The code to generate the random sets is shown in `iSIM_simulated_fps.ipynb`. The generation of the sets employs functions from `numpy`⁵² 1.24.2 and `random`⁵³ python packages.

For testing on real libraries, 30 ChEMBL29 curated datasets by van Tilborg *et al.*⁵⁴ were used (sets are available on https://github.com/molML/MoleculeACE/tree/main/MoleculeACE/Data/benchmark_data/old). The datasets had been curated by the authors using the default RDKit sanitation and outlier exclusion based on bioactivity.⁵⁴ Details of the set's size and corresponding targets are shown in Table S1.† The sets consisted of three binary fingerprint types, generated using RDKit:⁵⁵ RDKit⁵⁵ ($M = 2048$), MACCS⁵⁶ ($M = 167$) and ECFP4 (ref. 57) ($M = 1024$). All the continuous and discrete descriptors offered by the RDKit Descriptors⁵⁵ module were computed, descriptors with calculation errors or nan values were dropped for a total of 208 descriptors (for the full list, see the ESI†). Min max normalization was used prior to iSIM calculations.

Results

Average similarity

Our first tests were oriented towards checking the correspondence between the iSIM results and the average of the pairwise comparisons over a large number of libraries. For this, we used the 10 000 randomly generated libraries described in the previous section. As can be seen in Fig. 1, the iSIM results perfectly reproduce the more computationally demanding standard comparisons. In our previous contributions, we had only focused on the relation between the previously extended similarity results and the pairwise metrics as far as the ability of the extended indices to preserve the ranking of the comparisons (see, for example, Fig. 7 in ref. 23). The test presented in Fig. 1 is much more demanding, because we are comparing the similarity values obtained from both approaches. As noted in the Theory section, we expected the *iRR* and *iSM* results to be (analytically) identical to the pairwise averages. Even more remarkable, we see that *iT* provides a superb estimate for the $O(N^2)$ averages. This behavior is also observed over real datasets. In Fig. 2 we show a similar comparison, but now over 30 CHEMBL libraries, each represented by three different types of fingerprints. Fig. S1 and S2† include the same comparisons with more similarity index formulas that iSIM can be applied to.

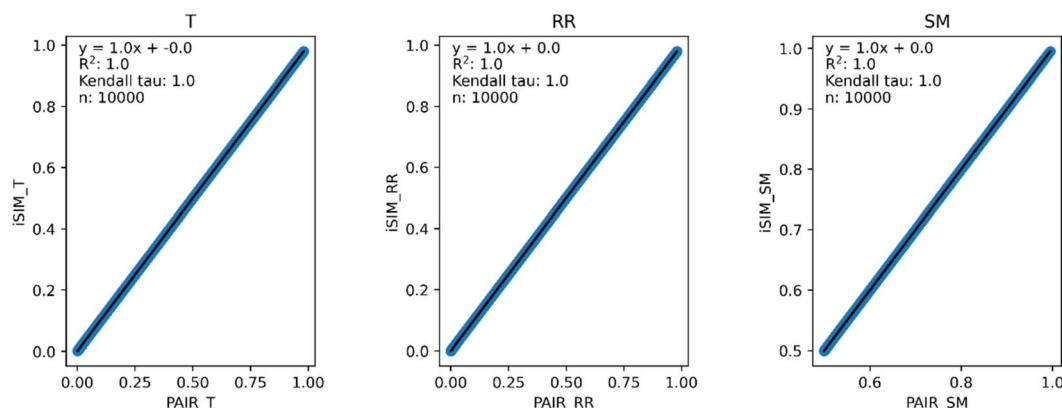


Fig. 1 iSIM vs. average pairwise similarity for 10 000 randomly generated libraries. Molecules are represented by binary fingerprints.

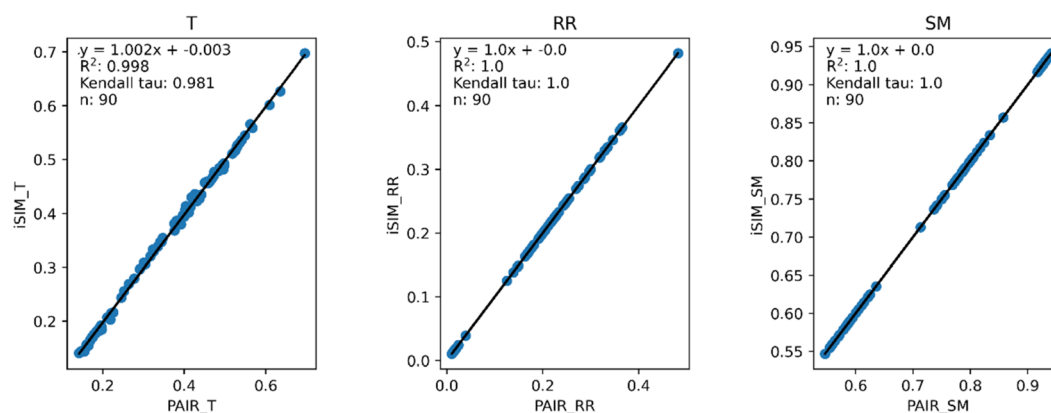


Fig. 2 iSIM vs. average pairwise similarity for 30 CHEMBL libraries. Molecules are represented by binary MACCS, RDKit, and ECFP4 (binary) fingerprints.



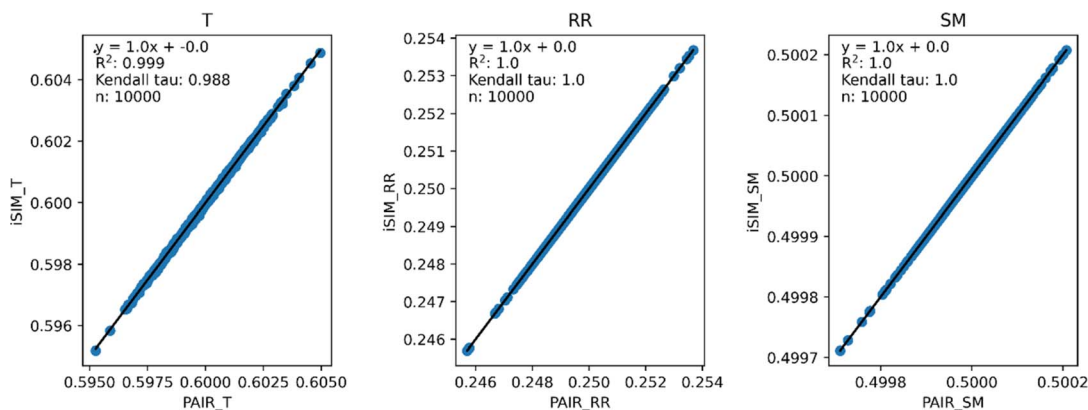


Fig. 3 iSIM vs. average pairwise similarity for 10 000 randomly generated libraries. Molecules are represented by random generated fingerprints with continuous normalized descriptors.

Fig. 3 and 4 present the equivalent results, but for molecules represented by (normalized) descriptors (*e.g.*, continuous real values). Once again, *iRR* and *iSM* show a perfect agreement both for the randomly generated and for the real data. The median approximation in *iT* is also remarkably robust over continuous data, essentially operating at as close a level as for the binary fingerprints.

Local analysis of molecular libraries

Complementary similarity. Complementary similarity calculations can also be applied with iSIM, as they were previously applied using extended similarity. One molecule is taken out of the set, and iSIM is calculated on the remaining compounds. In this way, low values will correspond to molecules that inhabit high density regions in chemical space. Conversely, high complementary similarity corresponds to molecules from low density regions, and thus, overall, least similar to the rest of the set. This tool enables a ranking of molecules on how similar they are to the rest of the set; the most similar molecule, the medoid, has the lowest complementary similarity and at the end of the ranking we will have the outlier.³⁹ As an example in Fig. 5, medoid and outlier molecules

from a dataset can be identified doing the complementary similarity ranking. Since we have a ranking of the molecules, the medoid and outlier cutoff can be flexible depending on the user needs; this gives an opportunity for visualization of relevant structures for the set. The information contained in the complementary similarity ranking has proven to be very valuable in stratifying the data as a pre-processing step in clustering,³⁹ as well as a way to quickly sample different regions of chemical space.⁴⁷

Diversity selection. To further expand on the applicability of iSIM, we focused on the classical cheminformatics task of sampling a given library in the most diverse way possible: the diversity picking problem. Just like the extended indices before, iSIM naturally leads to a diversity selection algorithm (iSIMDiv):

Pick a molecule and add it to the selected set. (This is usually done at random, but in order to increase the reproducibility of our results, in all cases we start from the medoid of the set.)

At every step, pick the molecule that will result in the lowest iSIM for the selected set.

As shown in Fig. 6A, this simple recipe leads to more diverse sub-sets than the popular MaxMin diversity selection algorithm.^{58,59} There, we tested the performance of these algorithms

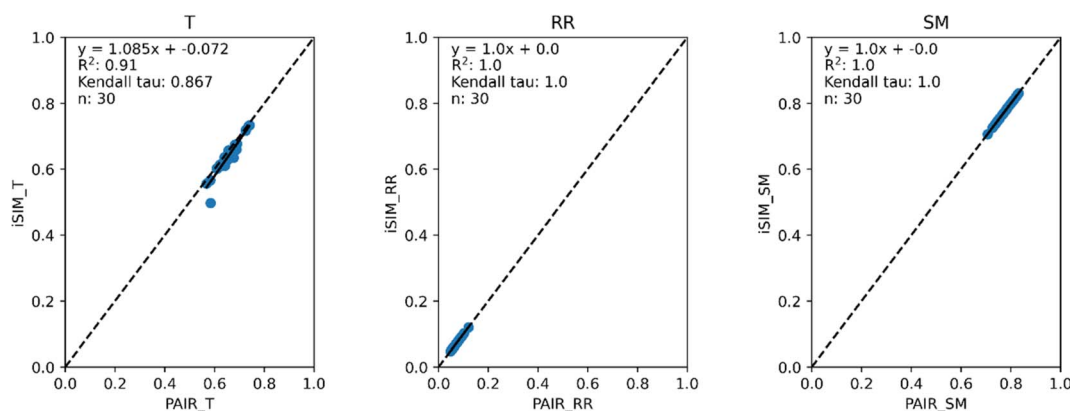


Fig. 4 iSIM vs. average pairwise similarity for 30 CHEMBL libraries. Molecules are represented by 208 RDKit continuous and discrete numerical normalized descriptors.



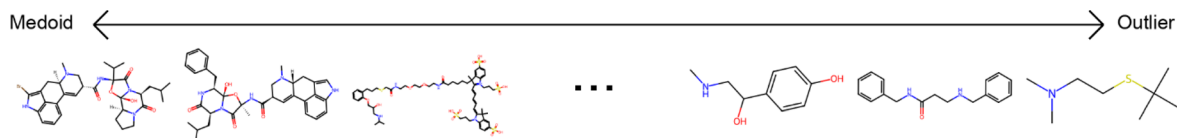


Fig. 5 Structures of the CHEMBL214 database ranked by increasing complementary similarity using the RDKit fingerprints and *iRR* similarity index. Structures shown correspond to the top (medoids) and bottom (outliers) three molecules.

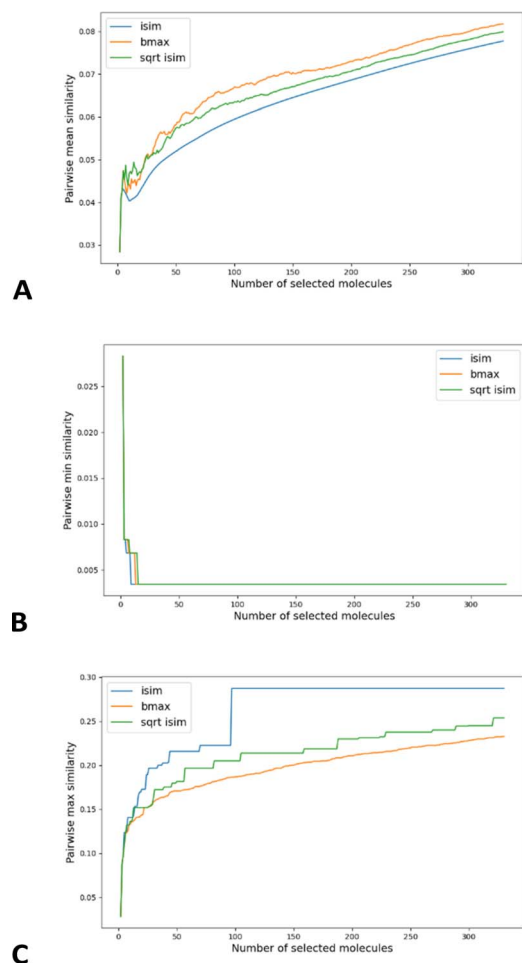


Fig. 6 MaxMin (bmax, yellow), *iRR* (iSIM, blue), and *sqrt_iRR* (sqrt_iSIM, green) results for the diversity sampling of the CHEMBL214 dataset represented by RDKit fingerprints: (A) pairwise similarity of the selected set, (B) minimum similarity between elements of the selected set, (C) maximum similarity between elements of the selected set.

over the CHEMBL214 library, corresponding to the 5-HT_{1a} receptor.⁵⁴ We selected a library with 3317 molecules (represented using RDKit fingerprints), and we monitored the process of selecting up to the 10% most diverse compounds. (The general trends observed for this library were corroborated for other libraries, similarity indices, and fingerprint types; see the ESI.†) If we quantify the chemical diversity of the selected set as inversely related to the average of the pairwise similarities of the molecules in the selected sub-set (the “y axis” in Fig. 5A), we see that iSIM (with the *iRR* metric), at worst, finds sets that are as diverse as those found by MaxMin with the standard

pairwise RR. This happens at the very early stages, when we have only picked a handful of molecules, but then quickly the iSIM results become more diverse. This is no surprise since, by definition, iSIM is constructed to reproduce the average of the pairwise comparisons. Hence, the iSIMDiv algorithm is directly maximizing this measure of chemical diversity.

If at the “global” or “coarse” level of the selected set it is clear that iSIMDiv produces more diverse sets, it is also interesting to study the “local” relations among the selected molecules. For instance, as shown in Fig. 6B, iSIMDiv is the algorithm that first finds a pair of “orthogonal” molecules in the data, that is, a pair of molecules with 0 similarity between them. On the other hand, we also see in Fig. 6C that iSIMDiv tends to produce selected sets where the closest pair of molecules is more similar to each other than the closest pair of molecules selected by MaxMin. This is in line with the properties of MaxMin, since this method tries to maximize the minimum distance between the new added molecule and those already selected. As a way to bridge the local gap between MaxMin and iSIMDiv we propose a version of iSIM that attempts to minimize not the sum of similarities, but the sum of the square roots of the similarities. This sqrt_iSIM can be easily calculated at the same cost as iSIM: for any iSIM variant, after calculating the sums of the columns of the molecular representations and generating the analogues of the *a*, *d*, and *b + c* indicators, we take their square roots and we use those in the same expression for the similarity indices. For example, in the case of *iRR*, we would be minimizing:

$$\text{sqrt}_i\text{RR} = \sqrt{\frac{2}{m}} \frac{1}{N(N-1)} \sum_{q=1}^m \sqrt{k_q(k_q - 1)} \quad (19)$$

As can be seen in Fig. 6C, minimizing this new objective function results in selected sets that are much locally closer to MaxMin, in the sense of having almost maximally dissimilar pairs of closest molecules. However, as reflected in Fig. 6A, this new sampling strategy also produces sub-sets that are more globally diverse than MaxMin (albeit not as diverse as those generated by iSIMDiv). In other words, by making changes to the objective function calculated within the iSIM framework, we can control the global and local properties of the sampled sets. Plots showing the same trends in the chemical diversity selection method for more databases, fingerprint representations and similarity indexes are included in the ESI.†

Another way of modifying the iSIM objective diversity metric that allows a faster diversity selection is what we called iSIM-RevDiv: iSIM reversed diversity selection. In this algorithm we start with all the points, and we iterate to find the molecule that,



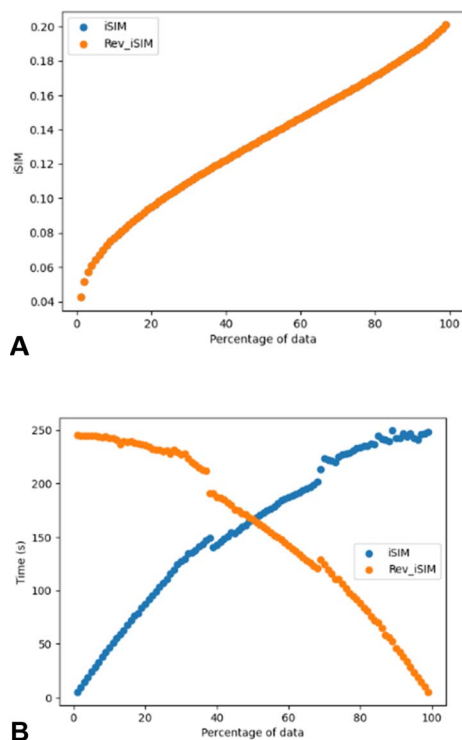


Fig. 7 (A) iSIMDiv and iSIMRevDiv selections for different data percentages (1–99%, in 1% steps) for the ChEMBL214 dataset represented by RDKit fingerprints and selected by the *i*RR index. (B) Computing time variation of the diversity selection methods with the data percentage selected.

if removed, would cause the remaining set to result in the lowest similarity value. This process is then repeated until the number of desired molecules is reached. iSIMRevDiv will be extremely useful in cases where more than 50% of the set wants to be picked. Fig. 7 shows the iSIM and computing time comparison between the iSIMDiv and iSIMRev methods for the ChEMBL214 database represented by RDKit fingerprints and using the *i*RR metric. Fig. 7A shows how when the diversity selection is started from the outlier, both forward and reversed iSIM diversity selection methods will yield the same average pairwise similarity results, which enables the user to use any of the two methods depending on the data percentage that wants to be picked. Fig. 7B shows computing times, and further supports the idea that for selections over 50% of the data the iSIMDivRev will be less computationally costly with the same high-quality results.

To further analyse the comparison of the iSIM diversity selection for both forward and reversed methods, random fingerprint datasets were generated, and the results were consistent with the ones previously observed (see Fig. S6†). The fact that diversity selection can be done in a reversed way makes iSIM diversity selection more attractive than typical algorithms like MaxMin where the computation of a pairwise similarity is required.

Up to this point, we have discussed algorithms that maximize the diversity (minimize the similarity) of the selected

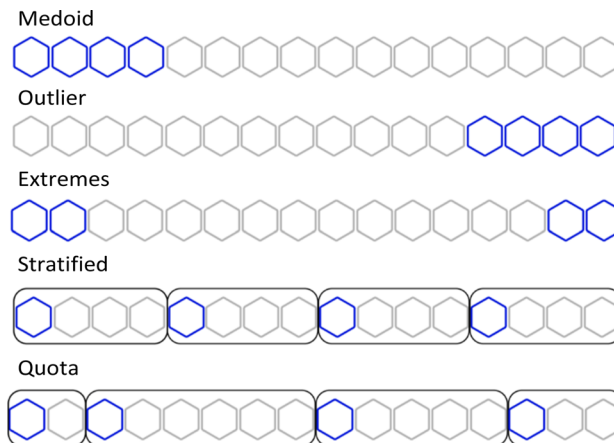


Fig. 8 Graphical explanation of the medoid, outlier, extreme, stratified and quota sampling methods.

molecules. However, if the goal is to pick a diverse set and to also cover the underlying chemical space, these presented methods are not the best approach. Algorithms like MaxMin and the iSIM diversity selection maximize the diversity by picking the periphery of the chemical space (molecules that are the least similar to the rest), at the expense of completely overlooking other sections of chemical space, resulting in a low coverage.⁶⁰

Using the complementary similarity, we can explore the chemical space with various approaches. Here, we propose five such methods. Fig. 8 shows graphically the explanation of each method. The first step for all the methods is to rank the molecules by increasing complementary similarity (as done in Fig. 5). After that, P molecules are selected based on the sector of the chemical space that wants to be sampled.

- Medoid sampling: the P with the lowest complementary similarity.
- Outlier sampling: the P with the highest complementary similarity.
- Extremes sampling: the $P/2$ with the lowest complementary similarity and the $P/2$ with the highest complementary similarity.
- Stratified sampling: molecules are separated into b strata of the same size, then molecules with the lowest complementary in each stratum are picked until P is chosen. The default number of strata is the same as the number of molecules to pick, hence one molecule per stratum is picked. If an equal number of molecules per stratum are needed, the priority will be the strata with lower complementary similarity.
- Quota sampling: the range of complementary similarity (max–min) is separated into b strata of equal range. Molecules are assigned to a stratum based on their complementary similarity; each stratum will have the same complementary similarity range but not necessarily the same number of molecules. The default number of strata is ten. Molecules are picked from each stratum until P is reached; priority to molecules and strata with lower complementary similarity is given.



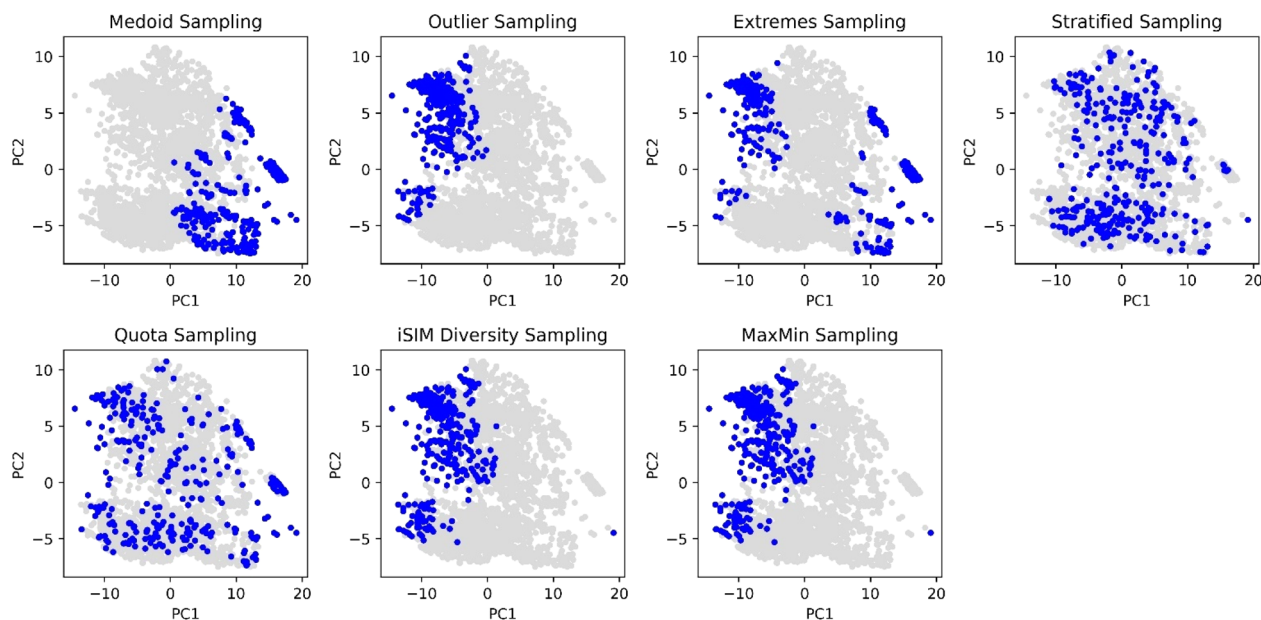


Fig. 9 PCA scoring plots of the ChEMBL214 dataset represented by RDKit binary fingerprints. Blue points represent the 10% selected molecules by each selection algorithm, while grey points represent non-selected molecules. iSIM related methods use t .

With the aim of comparing visually the selection methods proposed in this work, Principal Component Analysis (PCA)^{61,62} and t -Distributed Stochastic Neighbour Embedding (t -SNE)⁶³ plots were generated and 10% of the ChEMBL214 selected by each method is identified. The iSIM Tanimoto complementary similarity was used to perform the initial sorting step. In Fig. 9 it can be seen how the medoid and outlier sampling methods pick the extremes of the set's chemical space. Intuitively, medoids have high values for the PC1 scores, and the outliers lower values. As expected, the extremes sampling is a mix between the medoids' and outliers' areas. It is relevant to point out that the

iSIM diversity and MaxMin samplings pick molecules mostly from the same areas as the outlier sampling, proving the point that those algorithms maximize diversity but are not representative of the chemical space.

The selection methods that cover more of the chemical space are the stratified and quota samplings, with points spread through the two-dimensional space representation. Thus, if representativity is an important matter, we recommend these methods. Certain differences can be noticed between the two of them, the main one is that quota sampling includes more of the medoid and outlier regions than the stratified approach. The

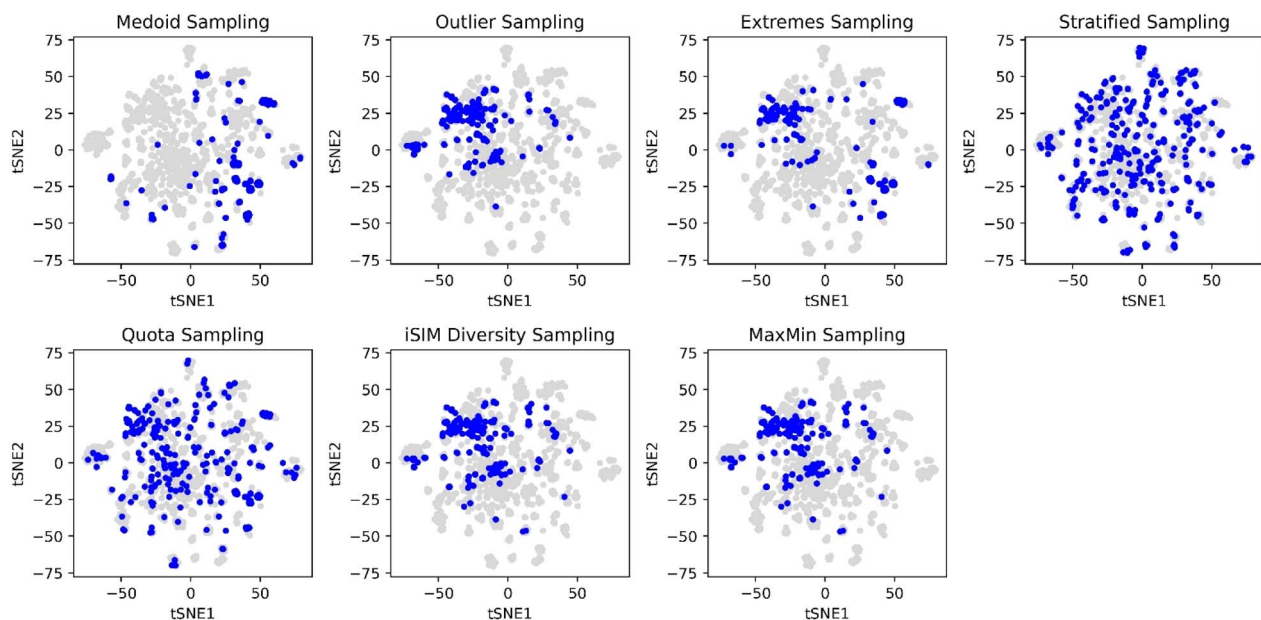


Fig. 10 t -SNE plots for the ChEMBL214 dataset represented by RDKit binary fingerprints. Blue points represent the 10% selected molecules by each selection algorithm, while grey points represent non-selected molecules. iSIM related methods use the t similarity index as a metric.

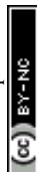


Table 1 $\bar{i}T$ values for 10% selected molecules by each sampling method for the ChEMBL214 dataset

Sampling method	$\bar{i}T$
Medoid	0.52405
Outlier	0.21217
Extreme	0.33403
Stratified	0.33066
Quota	0.32896
iSIM diversity	0.20132
MaxMin	0.20132
Complete dataset	0.33036

same trend in observations for the PCA was observed in the tSNE plots in Fig. 10.

Table 1 includes the iSIM ($\bar{i}T$) values of the selected molecules by each method. Notice how the average similarities for the diversity and MaxMin methods are the lowest, which is the purpose of their algorithms. The outlier method has a closer similarity value to the MaxMin and diversity sampling, suggesting that they sample around the same area of the chemical

space. The medoid sampling has the highest average similarity value, meaning that the molecules that are in the medoid area are highly similar. This could be an important tool to identify the “core” of a dataset. The values for extreme, stratified and quota are close to 0.33 which is the value for the whole set. For the quota and stratified methods this means that the selected molecules represent well the set, leading to an average similarity close to the complete set, supporting the visualization from previous figures. On the other hand, in the case of the extreme sampling this value is just a combination of two factors: low similarity values given by sampling from the extrema of the set compensated for by high similarity values whenever one is sampling within the outlier or the medoid region, resulting in a deceptively “average” iSIM value.

Clustering

As a final proof-of-principle demonstration of the versatility of the iSIM framework, we look at the clustering of molecular libraries. While there are many ways in which the notion of comparing multiple elements at the same time could be applied

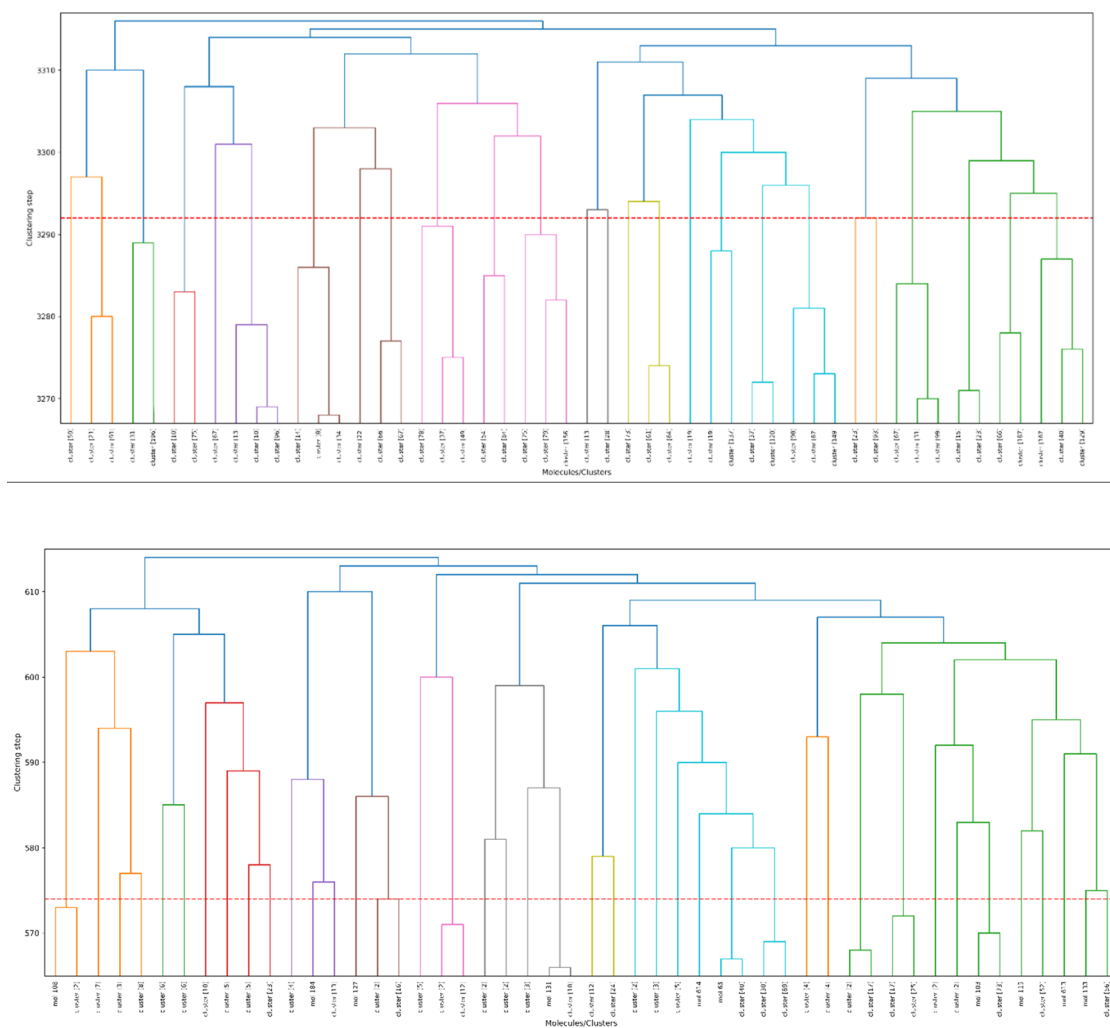


Fig. 11 Dendrograms from hierarchical clustering of molecules in the ChEMBL214 (top) and ChEMBL2835 (bottom) libraries using iSIM on MACCS fingerprints. The number of elements in each cluster is indicated in brackets. Coloring corresponds to the final 10 clusters. The dashed red line represents the cut-off for the optimal number of clusters (25 for ChEMBL214, 41 for ChEMBL2835).



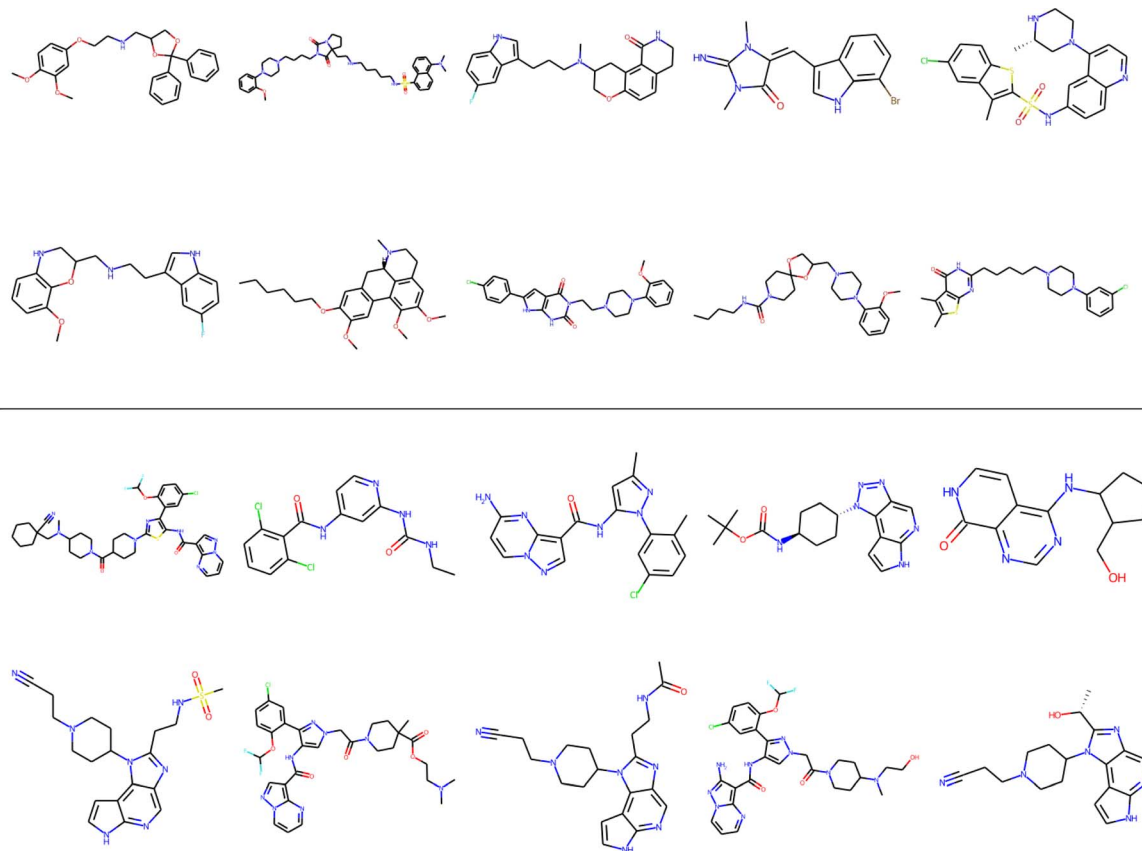


Fig. 12 Medoids of each of the 10 colored clusters in the CHEMBL214 (top) and CHEMBL2835 (bottom) libraries using *i*SIM on MACCS fingerprints.

to clustering problems, perhaps the most natural one is in the context of hierarchical agglomerative (HA) algorithms. Note that *i*SIM can be used as a linkage criterion in the sense that at any given point we can choose to combine the two sets that produce the largest *i*SIM value for their union. In more mathematical terms, given sets c_1, c_2, \dots, c_K , we combine clusters i, j such that: $i, j = \operatorname{argmax}_{p,q} i\text{SIM}(c_p \cup c_q)$. This is the criterion that we used in Fig. 11 to cluster the CHEMBL214 ($N = 3317$) and CHEMBL2835 ($N = 615$) libraries (using *i*SIM and MACCS fingerprints). We can also use the computed *i*SIM values to determine the optimum number of clusters in the data. If we follow the evolution of $i\text{SIM}_k$ (the *i*SIM of the cluster formed in the k th step) we see that this quantity will tend to decrease with increasing k , but it will tend to reach some “stability” when an optimum separation of the data is achieved. In other words, we look for the largest value of k for which the quantity $|i\text{SIM}_{k+1} - i\text{SIM}_k|$ is as close to 0 as possible.

Finally, clustering can be used to navigate through the molecular library, identifying representative structures associated with different basins in chemical space. For example, in Fig. 12 we show the medoids of the CHEMBL214 and CHEMBL2835 libraries in the case in which one selects 10 clusters in each of them. Note how our clustering is able to identify well-defined regions of chemical space that correspond to distinct scaffolds and functional groups. These structures, however, should not be mistaken for the most diverse structures

in the original library. (A common practice in some fields tends to identify the cluster centroids with a diverse representation of the set.) For instance, if we calculate the *i*SIM for the set of medoids when one has a number of clusters equal to 10% of the total number of points, we get 0.766 and 0.810 for CHEMBL214 and CHEMBL2835, respectively, which is far from a maximally diverse set. That is, if the *i*SIMDiv and MaxMin tend to sample the data by increasing chemical diversity, the sampling through the medoids of the clusters offers a more “uniform” picture of the original set.

Conclusions

*i*SIM has the ability to perform the comparisons of multiple objects at the same time, irrespective of whether they are represented by binary fingerprints or real-value descriptors. The analytical mathematical operations behind *i*SIM and the evidence from randomly generated data and real molecule libraries show that the same exact value of average pairwise comparisons can be achieved for similarity indexes with the denominator equal to the length of the fingerprint, like RR and SM. In cases where the denominator is not equal to the length of the fingerprint, like T, *i*SIM still provides an exceptional approximation to the pairwise comparison average, highlighting the robustness of the median approximation theorem. This brings the two key advantages of *i*SIM: the much more



attractive linear scaling $O(N)$ compared to the traditional pairwise indices, and the greater simplicity (no need to define coincidence thresholds and weight functions) compared to our previous extended similarity indices.

We showed that iSIM can be used to calculate the complementary similarity of each of the molecules in the library and a ranking can be done to identify and visualize molecules as part of high-density or low-density regions. Different diversity selection methods using the proposed framework can be applied depending on the necessity. iSIMDiv and iSIMRevDiv methods were developed to have two alternatives that output the same diversity results but differ in computing times depending on the percentage of data to select, adapting to the user's necessities. The iSIM metric can also be modified depending on whether the diversity selection is wanted to be globally or locally coerced, which can be done taking the square root of the iSIM counters to select data that will have a lower maximum pairwise similarity. Remarkably, all the proposed diversity selection methods have the same or better quality than the commonly used MaxMin. Another application of our work is hierarchical clustering, as we can use iSIM as a clustering objective function to be maximized when combining two molecules/clusters. The change in iSIM for the new cluster per clustering step can also be used as a metric to determine the optimal number of clusters. Overall, iSIM provides a flexible and easy-to-use framework to analyse molecular libraries, but that could be easily adapted to any problems that use comparisons between objects (metabolomics, MD simulations, *etc.*).

Finally, we want to discuss the computational gains offered by iSIM. That is, having shown the excellent agreement between the iSIM and the pairwise comparisons, the remaining question is: how much does the new $O(N)$ algorithm help speed-up the comparison of large sets of molecules? For instance, the ChEMBL team reported that FPSim2 took ~ 12 hours to compare the 1 941 405 compounds in ChEMBL 27 using a single core in an i9 laptop (https://chembl.github.io/FPSim2/source/user_guide/sim_matrix.html). On the other hand, Eloy Félix made public an independent test on the 2 372 674 molecules in ChEMBL 33 set using iSIM, which took less than 4 seconds to complete the same task (https://github.com/eloyfelix/iSIM/blob/main/isim_avg_set_sim.ipynb). That is, even the (poorly optimized) code accompanying this manuscript is capable of vastly outperforming (highly optimized) implementations based on pairwise comparisons when it comes to quantifying the chemical diversity of large datasets.

Data availability

The software used to calculate the instant similarity indices, and all the other studies presented in the manuscript, can be found in <https://github.com/mqcomplab/iSIM>.

Author contributions

KLP: conceptualization, data curation, investigation, methodology, software, validation, visualization, writing – original draft, writing – review & editing. TDK: conceptualization,

investigation, methodology. RAMQ: conceptualization, investigation, methodology, funding acquisition, software, resources, supervision, writing – original draft, writing – review & editing.

Conflicts of interest

There are no conflicts to declare.

Acknowledgements

Research reported in this publication was supported by the National Institute of General Medical Sciences of the National Institutes of Health under award number R35GM150620. We thank Eloy Félix for his help with the ChEMBL timing benchmark, and Patrick Walters for his insightful remarks.

References

- 1 E. Fernández-de Gortari, C. R. García-Jacas, K. Martínez-Mayorga and J. L. Medina-Franco, *J. Cheminf.*, 2017, **9**, 9.
- 2 R. Todeschini and V. Consonni, *Handbook of Molecular Descriptors*, Wiley, 2000.
- 3 S. Gugler and M. Reiher, *J. Chem. Theory Comput.*, 2022, **18**, 6670–6689.
- 4 P. Jaccard, *New Phytol.*, 1912, **11**, 37–50.
- 5 D. J. Rogers and T. T. Tanimoto, *Science*, 1960, **132**, 1115–1118.
- 6 R. Todeschini, V. Consonni, H. Xiang, J. Holliday, M. Buscema and P. Willett, *J. Chem. Inf. Model.*, 2012, **52**, 2884–2901.
- 7 M. A. Johnson, G. M. Maggiora, *et al.*, *Concepts and applications of molecular similarity*, Wiley-Interscience, 1st edn, 1990.
- 8 G. Hu, G. Kuang, W. Xiao, W. Li, G. Liu and Y. Tang, *J. Chem. Inf. Model.*, 2012, **52**, 1103–1113.
- 9 V. Zoete, A. Daina, C. Bovigny and O. Michielin, *J. Chem. Inf. Model.*, 2016, **56**, 1399–1404.
- 10 H. Eckert and J. Bajorath, *Drug Discovery Today*, 2007, **12**, 225–233.
- 11 J. M. Cohen, J. W. Rice and T. A. Lewandowski, *ACS Sustain. Chem. Eng.*, 2018, **6**, 1941–1950.
- 12 B. A. Posner, H. Xi and J. E. J. Mills, *J. Chem. Inf. Model.*, 2009, **49**, 2202–2210.
- 13 X. Ning, H. Rangwala and G. Karypis, *J. Chem. Inf. Model.*, 2009, **49**, 2444–2456.
- 14 E. A. Helgee, L. Carlsson, S. Boyer and U. Norinder, *J. Chem. Inf. Model.*, 2010, **50**, 677–689.
- 15 W. P. van Hoorn and A. S. Bell, *J. Chem. Inf. Model.*, 2009, **49**, 2211–2220.
- 16 R. Buonfiglio, O. Engkvist, P. Várkonyi, A. Henz, E. Vikeved, A. Backlund and T. Kogej, *J. Chem. Inf. Model.*, 2015, **55**, 2375–2390.
- 17 D. Stumpfe and J. Bajorath, *J. Med. Chem.*, 2012, **55**, 2932–2942.
- 18 M. P. Krein and N. Sukumar, *J. Phys. Chem. A*, 2011, **115**, 12905–12918.



- 19 D. J. Huggins, A. R. Venkitaraman and D. R. Spring, *ACS Chem. Biol.*, 2011, **6**, 208–217.
- 20 G. M. Downs, P. Willett and W. Fisanick, *J. Chem. Inf. Comput. Sci.*, 1994, **34**, 1094–1102.
- 21 P. Kovács, F. Tran, A. Hanbury and G. K. H. Madsen, *J. Chem. Theory Comput.*, 2022, **18**, 441–447.
- 22 G. Maggiora, M. Vogt, D. Stumpfe and J. Bajorath, *J. Med. Chem.*, 2013, **57**, 3186–3204.
- 23 G.-L. Xiong, Y. Zhao, L. Liu, Z.-Y. Ma, A.-P. Lu, Y. Cheng, T.-J. Hou and D.-S. Cao, *J. Med. Chem.*, 2021, **64**, 7544–7554.
- 24 B. Zhang, M. Vogt, G. M. Maggiora and J. Bajorath, *J. Comput.-Aided Mol. Des.*, 2015, **29**, 595–608.
- 25 D. Lemm, G. Falk von Rudorff and O. Anatole von Lilienfeld, *Machine Learning: Science and Technology*, 2023, **4**, 045043.
- 26 H. Ding, I. Takigawa, H. Mamitsuka and S. Zhu, *Briefings Bioinf.*, 2014, **15**, 734–747.
- 27 H. Safizadeh, S. W. Simpkins, J. Nelson, S. C. Li, J. S. Piotrowski, M. Yoshimura, Y. Yashiroda, H. Hirano, H. Osada, M. Yoshida, C. Boone and C. L. Myers, *J. Chem. Inf. Model.*, 2021, **61**, 4156–4172.
- 28 J. L. Bentley, *Commun. ACM*, 1975, **18**, 509–517.
- 29 J. H. Friedman, J. L. Bentley and R. A. Finkel, *ACM Transactions on Mathematical Software*, 1977, **3**, 209–226.
- 30 S. M. Omohundro, *Five Balltree Construction Algorithms*, International Computer Science Institute, 1989, pp. 1–22.
- 31 E. Felix, *chembl/FPSim2: simple package for fast molecular similarity searches*, <https://github.com/chembl/FPSim2>, accessed 4 February 2024.
- 32 A. Dalke, *J. Cheminf.*, 2019, **11**, 1–21.
- 33 D. K. Agrafiotis and V. S. Lobanov, *J. Chem. Inf. Comput. Sci.*, 1999, **39**, 51–58.
- 34 D. B. Turner, S. M. Tyrrell and P. Willett, *J. Chem. Inf. Comput. Sci.*, 1997, **37**, 18–22.
- 35 J. D. Holliday, S. S. Ranade and P. Willett, *Quant. Struct.-Act. Relat.*, 1995, **14**, 501–506.
- 36 R. A. Miranda-Quintana, D. Bajusz, A. Rácz and K. Héberger, *J. Cheminf.*, 2021, **13**, 32.
- 37 R. A. Miranda-Quintana, A. Rácz, D. Bajusz and K. Héberger, *J. Cheminf.*, 2021, **13**, 33.
- 38 J. Verhellen, *Chem. Sci.*, 2022, **13**, 7526–7535.
- 39 L. Chang, A. Perez and R. A. Miranda-Quintana, *Phys. Chem. Chem. Phys.*, 2022, **24**, 444–451.
- 40 A. Rácz, L. M. Mihalovits, D. Bajusz, K. Héberger and R. A. Miranda-Quintana, *J. Chem. Inf. Model.*, 2022, **62**, 3415–3425.
- 41 T. B. Dunn, G. M. Seabra, T. D. Kim, K. E. Juárez-Mercado, C. Li, J. L. Medina-Franco and R. A. Miranda-Quintana, *J. Chem. Inf. Model.*, 2022, **62**, 2186–2201.
- 42 R. Pikalyova, Y. Zabolotna, D. Horvath, G. Marcou and A. Varnek, *J. Chem. Inf. Model.*, 2023, **63**, 4042–4055.
- 43 E. A. Flores-Padilla, K. E. Juárez-Mercado, J. J. Naveja, T. D. Kim, R. Alain Miranda-Quintana and J. L. Medina-Franco, *Mol. Inf.*, 2022, **41**, 2100285.
- 44 T. B. Dunn, E. López-López, T. D. Kim, J. L. Medina-Franco and R. A. Miranda-Quintana, *Mol. Inf.*, 2023, **42**, 2300056.
- 45 A. Rácz, T. B. Dunn, D. Bajusz, T. D. Kim, R. A. Miranda-Quintana and K. Héberger, *J. Comput.-Aided Mol. Des.*, 2022, **36**, 157–173.
- 46 I. Redžepović and B. Furtula, *Mol. Diversity*, 2023, **27**, 1603–1612.
- 47 K. López-Pérez, E. López-López, J. L. Medina-Franco and R. A. Miranda-Quintana, *Molecules*, 2023, **28**, 6333.
- 48 P. F. Russell, T. R. Rao, *et al.*, *J. Malar. Inst. India*, 1940, **3**, 153–178.
- 49 R. R. Sokal and C. D. Michener, *University of Kansas science bulletin*, University of Kansas, 1958.
- 50 S. B. Guthery, *A motif of mathematics*, Docent Press, 2011.
- 51 E. R. Tou, *Math Horizons*, 2017, **24**, 8–11.
- 52 C. R. Harris, K. J. Millman, S. J. van der Walt, R. Gommers, P. Virtanen, D. Cournapeau, E. Wieser, J. Taylor, S. Berg, N. J. Smith, R. Kern, M. Picus, S. Hoyer, M. H. van Kerkwijk, M. Brett, A. Haldane, J. F. del Río, M. Wiebe, P. Peterson, P. Gérard-Marchant, K. Sheppard, T. Reddy, W. Weckesser, H. Abbasi, C. Gohlke and T. E. Oliphant, *Nature*, 2020, **585**, 357–362.
- 53 Random—generate pseudo-random numbers—Python 3.12.3 documentation, <https://docs.python.org/3/library/random.html>, accessed 17 April 2024.
- 54 D. van Tilborg, A. Alenicheva and F. Grisoni, *J. Chem. Inf. Model.*, 2022, **62**, 5938–5951.
- 55 RDKit, *RDKit: open-source cheminformatics*, <https://www.rdkit.org>.
- 56 J. L. Durant, B. A. Leland, D. R. Henry and J. G. Nourse, *J. Chem. Inf. Comput. Sci.*, 2002, **42**, 1273–1280.
- 57 H. L. Morgan, *J. Chem. Doc.*, 1965, **5**, 107–113.
- 58 F. Parreño, R. Álvarez-Valdés and R. Martí, *European Journal of Operational Research*, 2021, **289**, 515–532.
- 59 C. Kuo, F. Glover and K. S. Dhir, *Decision Sciences*, 1993, **24**, 1171–1185.
- 60 D. J. Woodward, A. R. Bradley and W. P. Van Hoorn, *J. Chem. Inf. Model.*, 2022, **2022**, 4402.
- 61 R. Bro and A. K. Smilde, *Anal. Methods*, 2014, **6**, 2812–2831.
- 62 G. Ivosev, L. Burton and R. Bonner, *Anal. Chem.*, 2008, **80**, 4933–4944.
- 63 L. der Maaten and G. Hinton, *Journal of Machine Learning Research*, 2008, 2579–2605.

